

Enter The DRAGON

Investigating the $^{13}\text{C}(p,\gamma)^{14}\text{N}$ reaction

Aaron Bebington

TRIUMF, 4004 Wesbrook Mall, Vancouver, British Columbia, Canada V6T 2A3 *

July 11, 2003

Interim report submitted to the Physics Department, University of Surrey
in partial fulfilment of the requirements of the degree of Master in Physics

Supervised by Professor J. D'Auria (TRIUMF), Professor P. Walker
(University of Surrey)



*Permanent address: Physics Department, University Of Surrey, Guildford, Surrey,
United Kingdom GU2 7XH

“Astrophysics has always been about the extremes of knowledge. Indeed, we look to the skies, in our hope to someday look down on the universe....”

Daniel West

Abstract

The $^{13}\text{N}(p,\gamma)^{14}\text{O}$ reaction is very important for our understanding of explosive astrophysical sites, such as novae and supernovae. This reaction determines the conditions under which the CNO cycle changes to the Hot CNO cycle, the main process of energy generation in such sites.

Since ^{13}N is unstable, and is very close in mass to ^{13}C , the DRAGON recoil mass separator at TRIUMF will firstly study the $^{13}\text{C}(p,\gamma)^{14}\text{N}$ reaction so that its properties can be compensated for when studying the $^{13}\text{N}(p,\gamma)^{14}\text{O}$ reaction.

Early analysis showed that not all the ^{14}N recoils, from the $^{13}\text{C}(p,\gamma)^{14}\text{N}$ reaction, make it through the DRAGON to the end detector.

Acknowledgements

I would like to thank all the people below, who have helped me put this report together.

From TRIUMF: Dr Sabine Engel, Mike Lamey, and Dario Gigliotti. From the University of Surrey: Dr Jim Al-Khalili, Amy Bartlett, Elizabeth Cunningham, and Daniel West.

Special thanks go to: Dr Alison Laird (TRIUMF), for helping me choose this project for my Masters, and to Dr Chris Ruiz (TRIUMF), for closely supervising me through this project.

Contents

Abstract	iii
Acknowledgements	iv
Contents	v
List of Figures	vi
1 Introduction	1
2 Theory	3
2.1 The CNO Cycle	3
2.2 The HCNO Cycle	4
3 Experiment	6
3.1 TRIUMF	6
3.2 The DRAGON Facility	9
3.3 The Importance of the $^{13}\text{C}(p,\gamma)^{14}\text{N}$ reaction	14
4 Data Analysis	16
5 Further Analysis	24
6 Conclusion	32
References	33

List of Figures

1	Graphical representation of the CNO cycle.	4
2	The Hot CNO cycle.	5
3	A plan view of TRIUMF.	7
4	A 3D cut-away view of the ISAC experimental hall.	8
5	The DRAGON recoil mass separator.	9
6	The BGO array, (which surrounds the gas target), and the vacuum pumps.	11
7	The DRAGON, in all its glory!	13
8	Graphical representation of the energy levels in ^{14}N	15
9	Energy spectrum of the most energetic coincidence gamma rays, per event, for run 8161.	18
10	Fitting a gaussian curve to an energy peak.	19
11	Running run 8161 offline, changing the ODB to look at the sum of coincidence gamma rays.	20
12	a 2D energy spectrum (from run 8142) of ΔE vs E in the first anode of the ionization chamber.	22
13	Confirmation of recoils and leaky beam. a) attenuated beam tune, b)+d) normal run, c) recoil tune.	23
14	GEANT simulation of the probability of how many of the 8 MeV gammas are deposited in x amount of BGO crystal(s).	25
15	GEANT simulation of the BGO gamma array, looking west of the beam direction.	26
16	GEANT simulation of a 3D view of the BGO array.	27
17	An array showing which BGOs are next to each other.	28

18	The coincidence recoil spectrum for run 8142, a $^{13}\text{C}(\text{p},\gamma)^{14}\text{N}$ reaction with a incoming beam energy of 558 keV/u.	30
19	Monte Carlo simulation of the $^{13}\text{C}(\text{p},\gamma)^{14}\text{N}$ reaction with all the gammas plus cascades included, and an angular cut put on the recoils.	31

1 Introduction

Being a physicist means you ask questions about everything, but the more you learn and understand, the more and more questions there are to ask.

Questions like “Where did we come from?”, “Why is the world the way it is?”, “How were the atoms that make up our bodies made, and where were these atoms created?”, answers to which lie in understanding the nucleosynthesis of the chemical elements that make up the Universe.

The temperatures in the first three minutes after the Big Bang were hot enough for hydrogen nuclei to fuse together forming small quantities of heavier elements. However, this initial nucleosynthesis only accounts for the next two elements, (helium and a small amount of lithium), up to mass $A = 7$. So how was man, and our world containing elements up to the uranium region, created if this is true? The answers lie in the stars above. For centuries man has looked to the heavens for the truth. What we have found is an answer to where the other chemical elements came from.

Today, we are convinced that elements with mass $A > 7$ come from the nuclear reactions taking place in stars. Quiescent burning can account for some of the elements produced close to the valley of stability. In normal stellar conditions, unstable nuclei decay before they have the chance to react. However, in the high densities and hot temperatures of exploding stars, these decays can be bypassed by radiative proton and alpha capture reactions, whereby a lighter nucleus absorbs a proton or alpha forming an excited

state of a heavier nucleus, then releases the excess energy through gamma decay.

One site in the Universe where this happens is a nova. In this stellar binary system, a white dwarf star accretes hydrogen rich matter from a younger companion onto its surface. In the hydrogen rich layer on the white dwarf surface (which consists of oxygen and neon), high temperatures are reached leading to the ignition of nuclear fusion processes. This results in an explosion that forms elements up to silicon. Other stellar sites, such as supernovae and x-ray bursters, can produce even higher mass elements through the r-process, s-process, and rp-process.

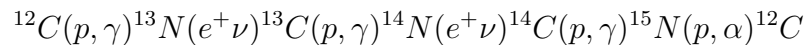
Physicists have modelled novae and have pointed out several important reactions that occur during the explosion which can greatly influence the rate of energy generation and the elements produced, and hence the overall course of the nova. More knowledge of these crucial reactions and their rates will lead us to a better understanding of stellar evolution, element creation, and eventually to the bigger questions of how the universe evolved and where the elements we are made up of were created.

An important reaction chain at the beginning of exploding novae is the CNO cycle. This report will look into the early analysis of the $^{13}\text{C}(p,\gamma)^{14}\text{N}$ reaction (which occurs in the CNO cycle) data obtained using the DRAGON recoil mass separator at TRIUMF's ISAC facility.

2 Theory

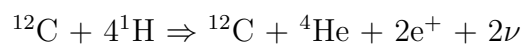
2.1 The CNO Cycle

In stars more massive than our Sun, with significant amounts of heavier elements (i.e. Population I stars), the main method of energy production is the fusion of hydrogen in the Carbon-Nitrogen cycle. The CN cycle uses these two elements as catalysts for a sequence of proton captures and beta decays for the production of helium (He). The cycle begins with the radiative proton capture on ^{12}C followed by further proton captures and beta decays:



The (p, α) reaction on ^{15}N ends the cycle because this reaction is more likely than another proton capture. As temperatures rise further to around 10^7 K [1], proton capture on ^{14}N becomes more probable than beta decay. This leads to the Carbon-Nitrogen-Oxygen (CNO) cycle:

Summing the particles before and after one cycle:



Like the CN cycle, the carbon, nitrogen and oxygen nuclei are used as catalysts with their relative abundances remaining unchanged. For both cycles, an initial amount of ^{12}C is required plus a hydrogen-rich environment. [1, 2, 3].

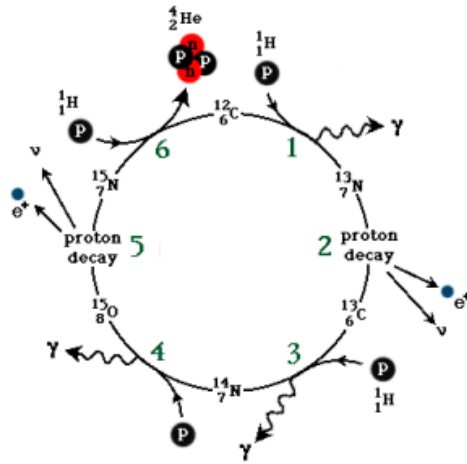


Figure 1: Graphical representation of the CNO cycle.

2.2 The HCNO Cycle

The ‘waiting points’ of the CNO cycle are the nuclei with the longest beta decay lifetimes. Here the cycle must wait for the element to beta decay, if the probability of proton capture is extremely low [1].

If the temperature gets high enough, in the range $0.1\text{-}1.5 \times 10^9$ K [4], proton captures become more probable. Therefore, in the same way the CN cycle transforms to become the CNO cycle by the proton capture reaction ${}^{14}\text{N}(p,\gamma){}^{15}\text{O}$ dominating over the beta decay of ${}^{14}\text{N}$, the ${}^{13}\text{N}(p,\gamma){}^{14}\text{O}$ reaction dominates the beta decay of ${}^{13}\text{N}$ transforming the CNO cycle into what is known as the “hot” CNO (HCNO) cycle.

There is no proton capture on ${}^{14}\text{O}$ and ${}^{15}\text{O}$ because the fluorine isotopes ${}^{15}\text{F}$ and ${}^{16}\text{F}$ are proton unstable [2]. This means that the rate of energy production is limited by these waiting points at ${}^{14}\text{O}$ and ${}^{15}\text{O}$ ($t_{1/2} = 70.6$ s and

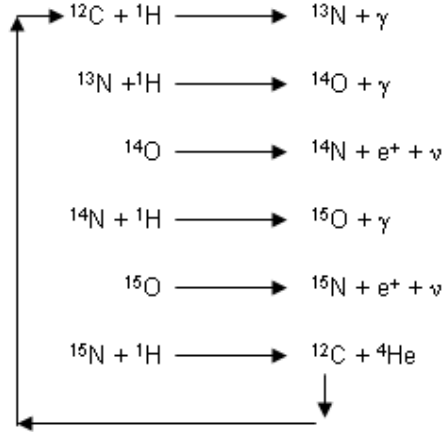


Figure 2: The Hot CNO cycle.

$t_{1/2} = 122.2$ s, respectively) [1]. The main product material from the HCNO cycle is ^{15}N due to the build up of ^{15}O , the isotope with the longest half life. This is helpful in distinguishing between the CNO and HCNO cycles, using the relative abundances of ^{14}N to ^{15}N . For the CNO cycle, [$^{14}\text{N} / ^{15}\text{N}$] is about 10^5 , but for the HCNO cycle this value is nearer 0.5 [2].

The HCNO cycle bypasses the beta decay of ^{13}N resulting in the cycle proceeding much quicker than the CNO cycle. The half life of ^{13}N is 9.97 minutes [5], while the half life of ^{14}O is 70.6 seconds. This implies a much larger production rate of helium, and more importantly, a higher energy generation rate.

Again, for this cycle there is an input of 4 protons and an output of 1 helium nucleus.

3 Experiment

3.1 TRIUMF

TRIUMF (TRI-University Meson Facility) is Canada's National Laboratory for Particle and Nuclear Physics, and is situated in Vancouver, on the University of British Columbia campus. It is one of three meson facilities in the world, and has the world's largest cyclotron. Within TRIUMF's cyclotron, negatively charged hydrogen ions reach energies up to 520 MeV. The acceleration of the ions by the cyclotron is caused by the repeated 'kicks' of electric voltage 23 million times per second. After 3000 kicks, the ions are moving at 75% of the speed of light¹. These intense beams of protons are directed out of the cyclotron into pipes (known as beam lines) which lead into experimental areas: the meson hall and the proton hall. In the meson hall, the beam strikes a solid target (carbon, beryllium, copper, or water) which knocks off short-lived pions (known as pi-mesons) from the target atom, which are studied in various experimental stations. In the proton hall, the beam is used directly for analysis and measurements of the properties of nuclei. [6]. (Figure 3).

A beam line is also directed to the ISAC (Isotope Separator and Accelerator) hall. ISAC produces a wide range of radioactive ion beams with intensities higher than at any other facility in the world. There are two experimental areas within ISAC: the low and high energy areas. The low en-

¹Beam energies can vary as low as 60 MeV up to 520 MeV. A moving stripping foil inside the cyclotron removes the two electrons from each negatively charged hydrogen ion and allows the remaining protons to channel out of the accelerator. Using more than one stripping foil allows up to three protons beams to be directed out of the cyclotron at the same time, each with different intensities and energies.

BEAM LINES AND EXPERIMENTAL FACILITIES

ISAC - I & ISAC - II EXPERIMENTAL HALLS

— PRESENT
 — FUTURE

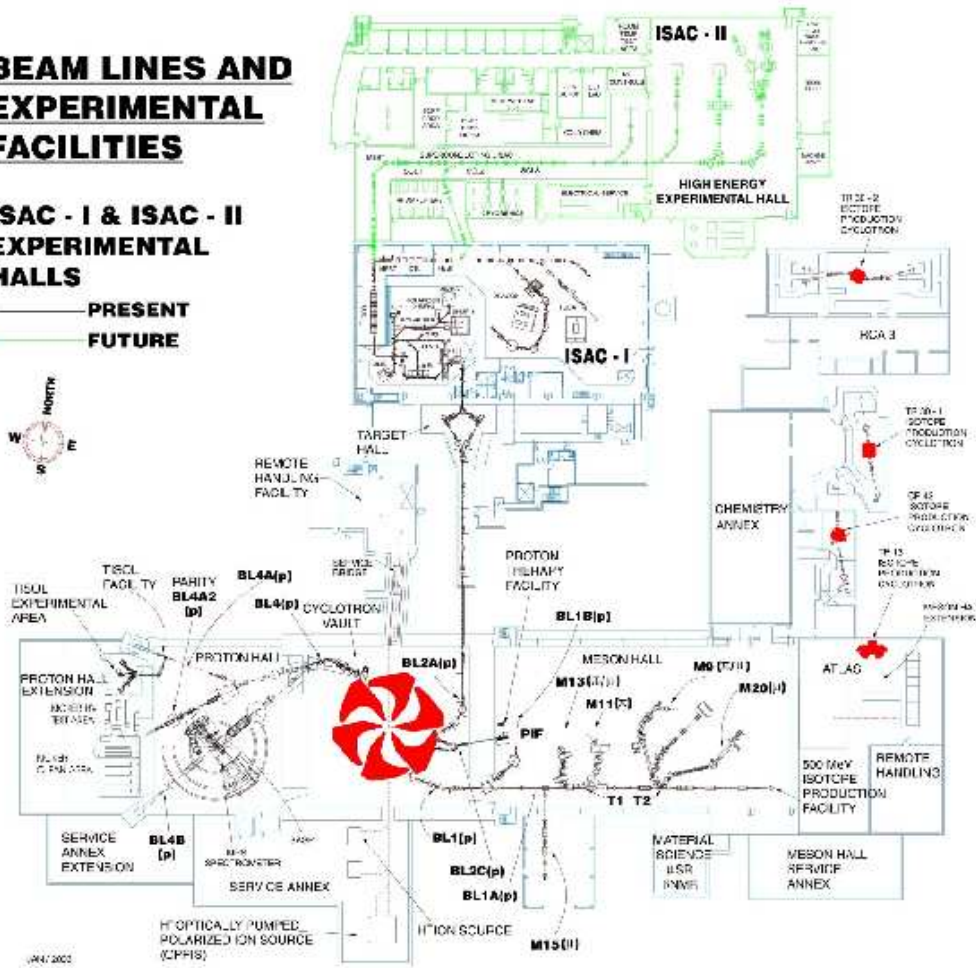


Figure 3: A plan view of TRIUMF.

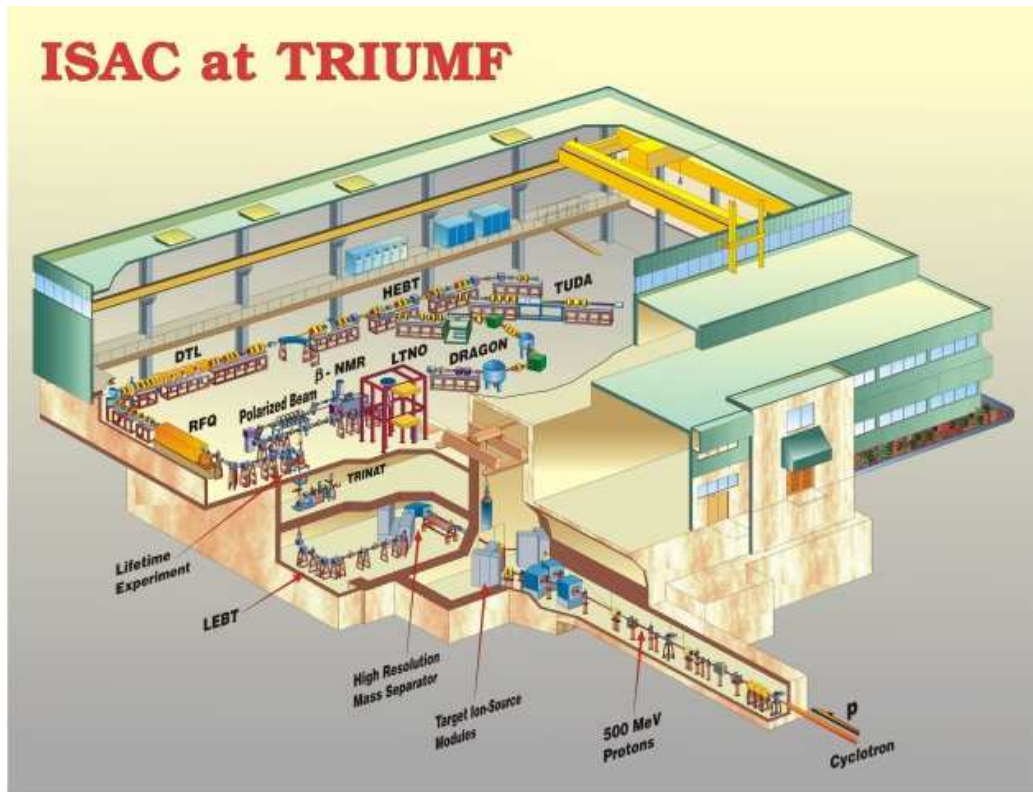


Figure 4: A 3D cut-away view of the ISAC experimental hall.

ergy area uses a non-accelerated, mass separated heavy ion beam for studies in fundamental interactions, nuclear physics, and condensed matter physics. For the high energy area, the beam is passed through the two ISAC accelerators: RFQ (Radio Frequency Quadrupole) and DTL (Drift Tube Linac). Here, beams of masses below 30 amu can be accelerated to energies from 0.15 - 1.5 MeV per mass unit, and are sent in pulses of 1 per 86 nano-seconds to the high energy experiments. This range of energies is the optimal range for studies into the understanding of explosive nucleosynthesis and nuclear astrophysics as a whole, leading to explanations of the evolution of chemical elements in the universe. [7, 8]. (Figure 4).



Figure 5: The DRAGON recoil mass separator.

3.2 The DRAGON Facility

DRAGON (Detector of Recoils And Gammas Of Nuclear reactions) [9, 10, 11] is on the high energy beam line from the cyclotron at the TRIUMF-ISAC facility, and was designed to measure radiative capture reactions in inverse kinematics using a hydrogen or helium gas target [8]. The DRAGON system (see figure 5) is basically a 21m recoil mass spectrometer² which can create elements via proton or alpha capture reactions and then separate them based on mass. This is achieved in two stages.

²21m from the target center to the end detector.

The first stage of DRAGON consists of a windowless gas target, which has a 12.3 cm effective length. A series of pumps are found either side of the entrance and exit to the target, and are used to keep the beam line in a (near) perfect vacuum by removing any gas that may leak out of the target. This allows the beam to pass cleanly through the target. Surrounding the target is a closely-packed array of 30 gamma detectors made of BGO (Bismuth Germanium Oxide) scintillation crystals. These detect the gamma rays emitted in the nuclear reaction within the gas and measure their energies³. (Figure 6).

On leaving the gas target, the products (or ‘recoils’) of the nuclear reaction, plus the original beam, enter the second stage of DRAGON: the mass spectrometer. The mass spectrometer is made up of a series of magnetic dipoles (M), magnetic quadrupoles (Q), magnetic sextupoles (S), and electrostatic dipoles (E), and they are arranged in a two stage mass separation: (QQMSQQQSE)(QQSMQSEQQ). The magnetic dipoles use a magnetic field to separate ions by their charge state through different amounts of curvature (Eq. 1). The dipoles are set in such a way that it bends the charge state of interest through the charge state slits, while all other charge states are stopped inside the charge slit box.

³When a gamma ray enters the BGO crystal, it reacts with an atom inside. This reaction excites an electron to an excited state, and as the excited electron falls back down to a lower energy state it releases its energy in the form of a photon. This is repeated for each atom the gamma ray interacts with, in the BGO, losing some energy each time. The total sum of light (i.e photons) is read by a PMT (Photo-Multiplier Tube) attached at the end of the BGO crystal. The sum of light is proportional to energy of the gamma ray. [12]

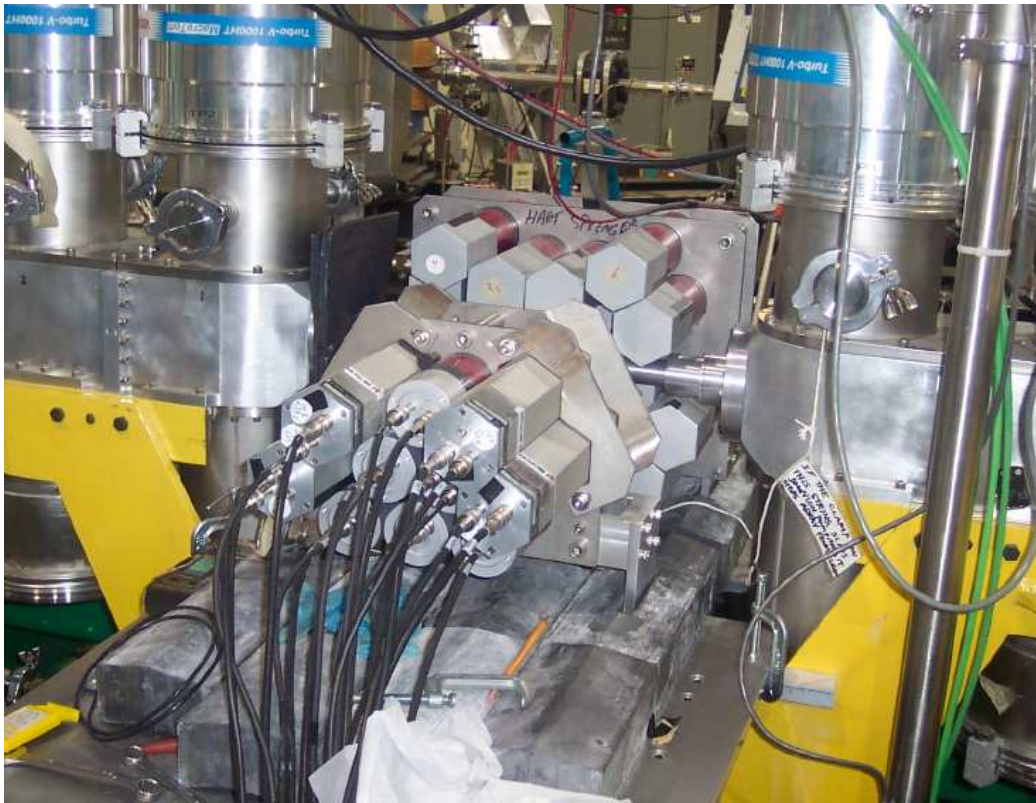


Figure 6: The BGO array, (which surrounds the gas target), and the vacuum pumps.

$$r = \frac{mv}{Bq} \quad (1)$$

The beam and recoil ions leave the magnetic dipoles and carry on downstream with the selected charge state. They have the same momentum and will therefore have different velocities (Eq. 2), and hence, different kinetic energies (Eq. 3). The kinetic energy of the recoils is chosen, and the appropriate voltage is applied to the electric dipoles such that the recoils pass through the separator, and the beam ions are stopped. The ions then pass through another magnetic and electric dipoles (MD2 and ED2 respectively) to improve the suppression of beam ions with respect to recoil ions.

$$p = mv \quad (2)$$

$$E = \frac{1}{2}mv^2 \quad (3)$$

Currently DRAGON has four main end detectors: a double sided silicon strip detector (DSSSD), a micro-channel plate (MCP), a parallel grid avalanche counter (PGAC), and an ionization chamber (IC). They can be used individually or in combination, depending on the type and precision of the data required.

The DSSSD gives data on the number of ions detected, the energy the ions hit the detector with, and the position of the ions on the focal plane. The DSSSD consists of 16 front strips and 16 back strips. Each strip is 3 mm wide, which provides a (256 x 3) mm² pixel area on a 5 cm² detector, giving the x-y position data. [13].

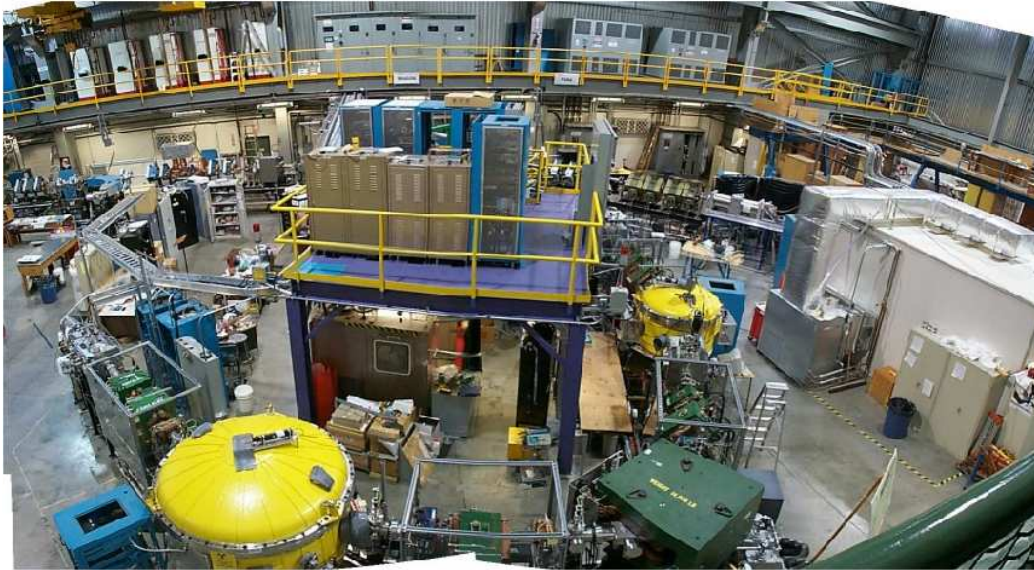


Figure 7: The DRAGON, in all its glory!

The MCP and PGAC are used to provide two timing signals from which the time of flight of the ion can be deduced. The MCP, when used with the DSSSD, can also give the number of counts as well as position. The PGAC, when used with the IC, was designed to give values of position and time. The PGAC is an ionization detector consisting of an anode sandwiched between two cathodes. The two cathodes provide the position information. Each cathode is a plane of wires at right angles to the other, thus giving an x and y position. The anode gives the timing signal. [14].

The IC gives a timing signal, the number of counts, and can distinguish particles by their mass.

3.3 The Importance of the $^{13}\text{C}(\text{p},\gamma)^{14}\text{N}$ reaction

The ^{13}N nuclide is very important in the CNO cycle. It is this element that will either beta decay to ^{13}C following the CNO cycle, or proton capture to form ^{14}O changing the flow to the Hot CNO cycle. This is important for our understanding of novae and supernovae. ^{13}N takes approximately 10 minutes to beta decay, but if the temperature is hot enough, ^{13}N will capture a proton to form ^{14}O , which then beta decays in approximately 70 seconds. This means that the HCNO cycle is much faster and has a higher rate of production of energy. This leads to H and He burning faster, thus resulting in a nova. Consequently the temperature for which there is a change from the CNO to the HCNO cycle is important for our understanding of novae. So what is the relevance of $^{13}\text{C}(\text{p},\gamma)$?

^{13}N and ^{13}C are very close in mass, in fact they are the two closest mass related elements. ^{13}N is not a stable element (unlike ^{13}C), and because of their small mass difference, a ^{13}N beam will contain ^{13}C as well. This means that there will be ^{14}N recoils with the ^{14}O recoils from the ^{13}N , as well as ^{13}C and ^{13}N leaky beam.

Understanding the $^{13}\text{C}(\text{p},\gamma)^{14}\text{N}$ reaction means we can compensate for the ^{14}N recoils and ^{13}C leaky beam⁴ for the important $^{13}\text{N}(\text{p},\gamma)^{14}\text{O}$ reaction.

⁴leaky beam - a term to describe unreacted incoming beam that makes it through the DRAGON to the end detector with the recoils.

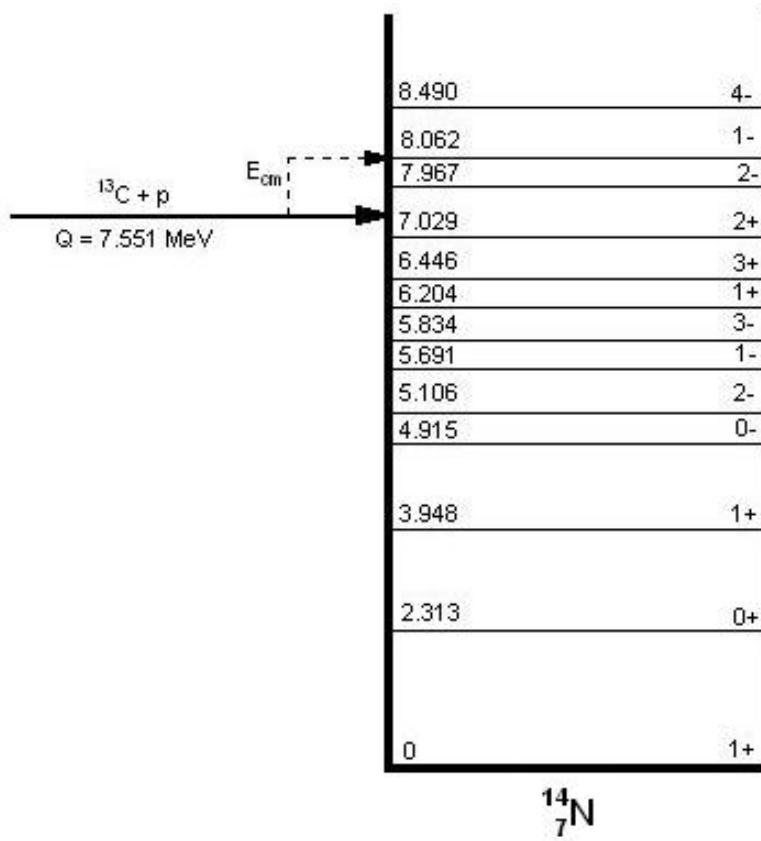


Figure 8: Graphical representation of the energy levels in ^{14}N .

4 Data Analysis

The analyzer used for DRAGON is a MIDAS⁵ program which runs: a) online as part of the data acquisition (DAQ), and b) offline to analyze old event-by-event .mid files. This MIDAS analyzer operates as a pipeline to make histograms from event-by-event data, to write these histograms into .hbook (online) or .rz (offline) files, and use PAW++⁶ for histogram display. [16]

An offline event stream from the .mid file can be passed through the analyzer many times, making offline analysis different from online analysis where the online event stream can only pass once through the analyzer. Each time the offline event stream is passed through, changes to the ODB (Online Data Base) are made to eliminate more and more unwanted background events. Final changes to the ODB are saved to document the complete analysis. [16]

For example, figure 9 shows the spectrum 1001 from the online .hbook file of run number 8161. This $^{13}\text{C}(p,\gamma)$ run lasted for 1700 seconds, and had an incoming beam energy of 543.8 keV/u. Using Eq. 4, the Q-value for this reaction is 7.551 MeV. Eq. 6 gives the center-of-mass energy (E_{cm}). For run 8161 this was 508.6 keV. Eq. 8 gives the excitation energy (E_x) of the gamma emitted from this reaction. For run 8161, this was 8060 keV.

⁵Maximum Integrated Data Acquisition System - a general purpose system, developed at TRIUMF and the Paul Scherrer Institute (Switzerland) between 1993 and continuing to this day, for event based data acquisition in small to medium scale physics experiments [15].

⁶Physics Analysis Workbench - a general purpose portable tool for analysis and presentation off physics data.

$$Q = \Delta mc^2 \quad (4)$$

where:

$$\Delta m = m(^{13}\text{C}) + m(^1\text{H}) - m(^{14}\text{N}) \quad (5)$$

$$E_{cm} = \mu E_{beam} \quad (6)$$

where:

$$\mu = \frac{mM}{m + M} \quad (7)$$

$$E_x = Q + E_{cm} \quad (8)$$

Therefore, a coincidence⁷ gamma energy graph of this run will have a peak which is 8060 keV. As the energy x-axis of such a graph in PAW++ was not known, we can plot a Gaussian to the peak, and knowing the x-axis channel number, can find a calibration constant for this axis (see figure 10). Figure 10 is a plot of $c\gamma_0$ energy, where $c\gamma_0$ is the most energetic gamma detected at any given time in the BGO gamma detector array. The various other peaks will be cascade gammas to other excited states. Therefore, by summing up all the gamma cascades per event, will give, (for this run), the 8060 keV energy peak (see figure 11). This was done by running run 8161 offline and changing the title of the spectrum in the ODB. Also the x-axis has been changed so that only the relevant data is in the spectrum.

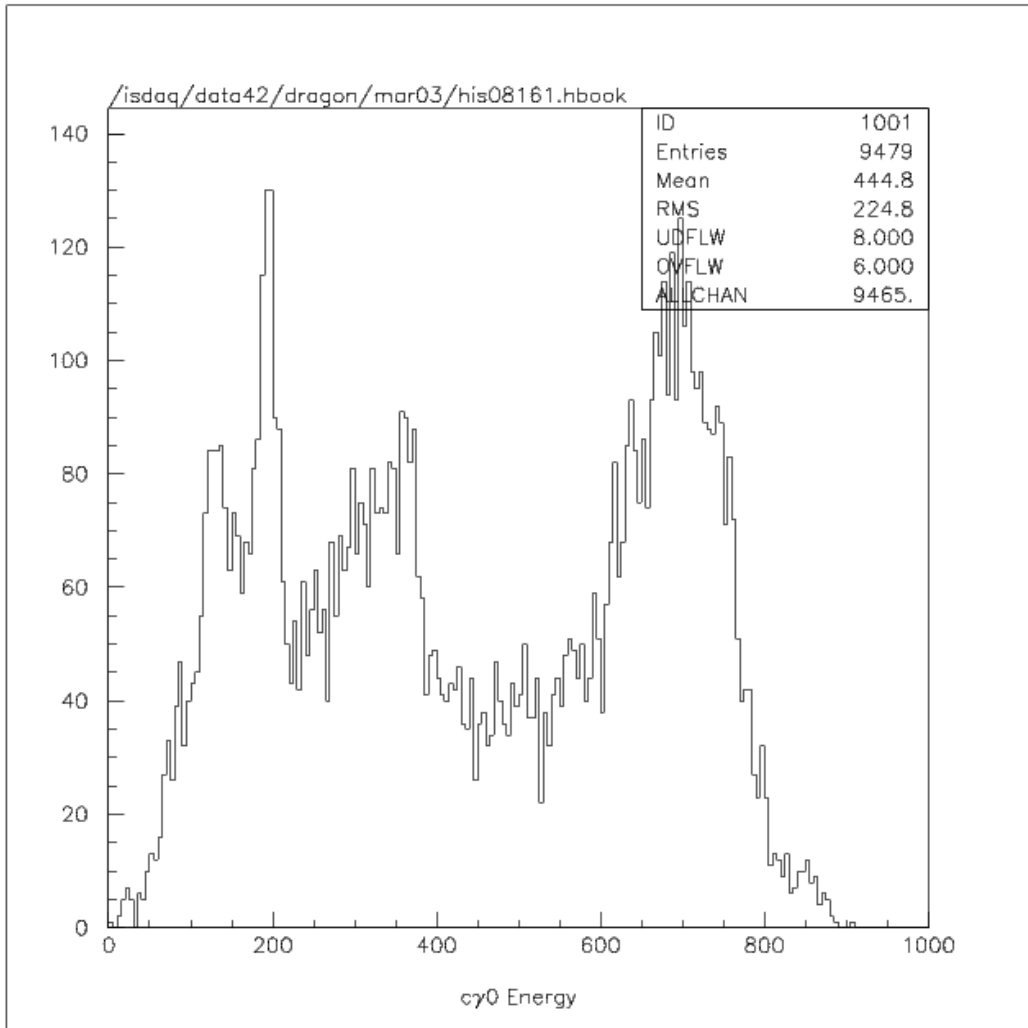


Figure 9: Energy spectrum of the most energetic coincidence gamma rays, per event, for run 8161.

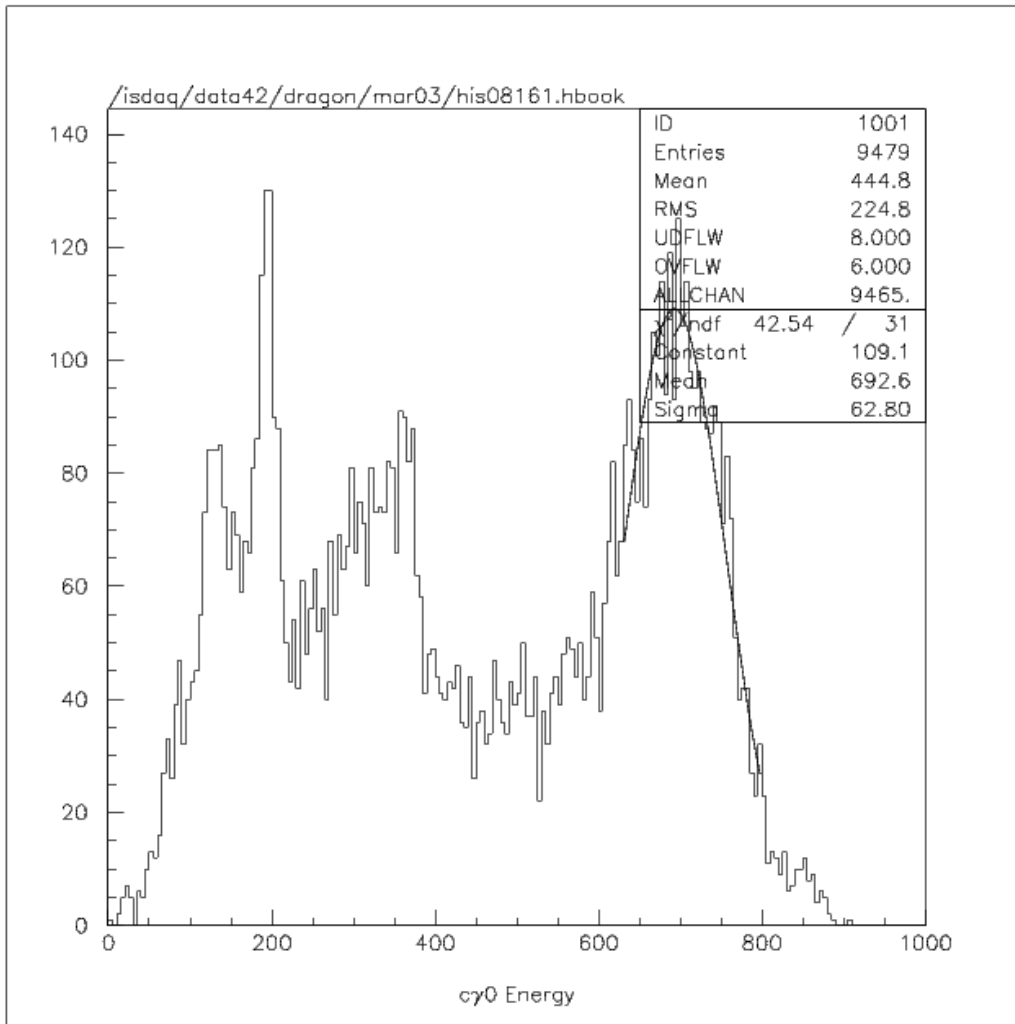


Figure 10: Fitting a gaussian curve to an energy peak.

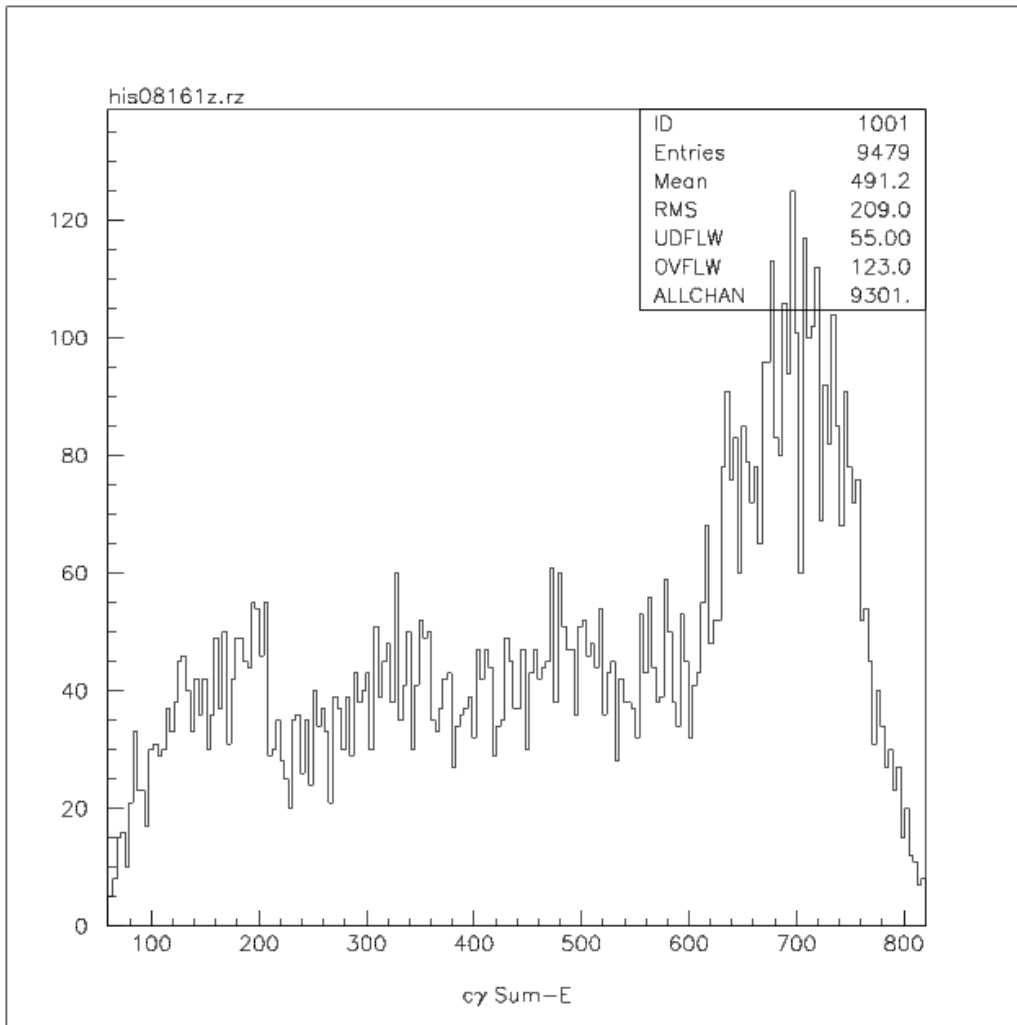


Figure 11: Running run 8161 offline, changing the ODB to look at the sum of coincidence gamma rays.

The ionization chamber is made up of four anodes. Looking at the energy spectrums, ΔE vs E , for the first anode in the ionization chamber (figure 12) we see that there may be leaky beam getting to the end detector. To check what is leaky beam and what is recoils, there were earlier recoil tunes and attenuated beam runs. Figure 13a shows an attenuated beam run, and figure 13c shows a recoil tune. Comparing these two runs to run 8142 (figure 13b) shows that the circle in figure 12 is actually leaky beam. Therefore, a cut can be made in further analysis, to only include the recoil data.

⁷i.e. the data that relates to a recoil heavy ion of ^{14}N as detected by the end detector.

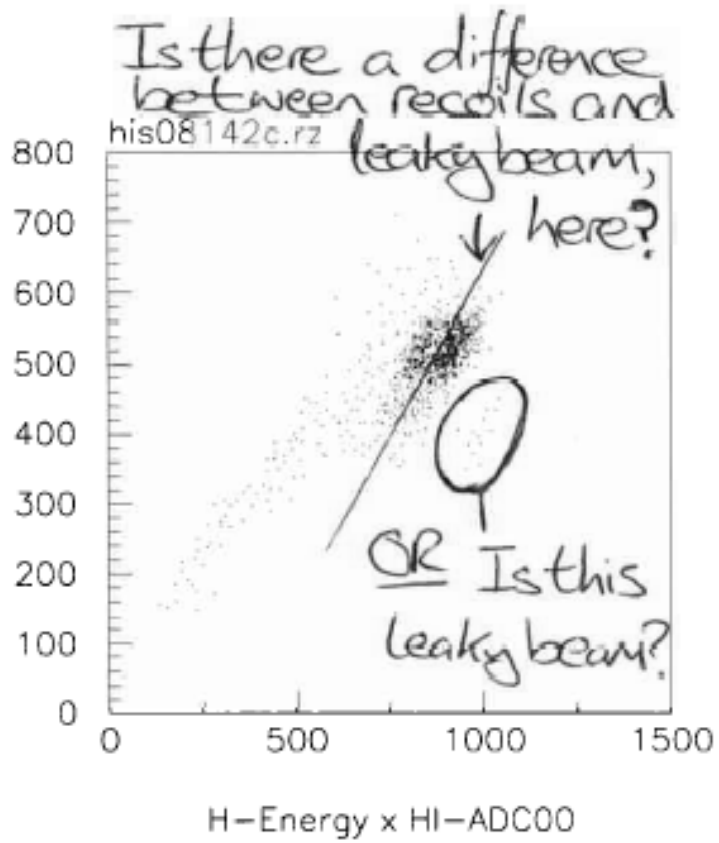


Figure 12: a 2D energy spectrum (from run 8142) of ΔE vs E in the first anode of the ionization chamber.

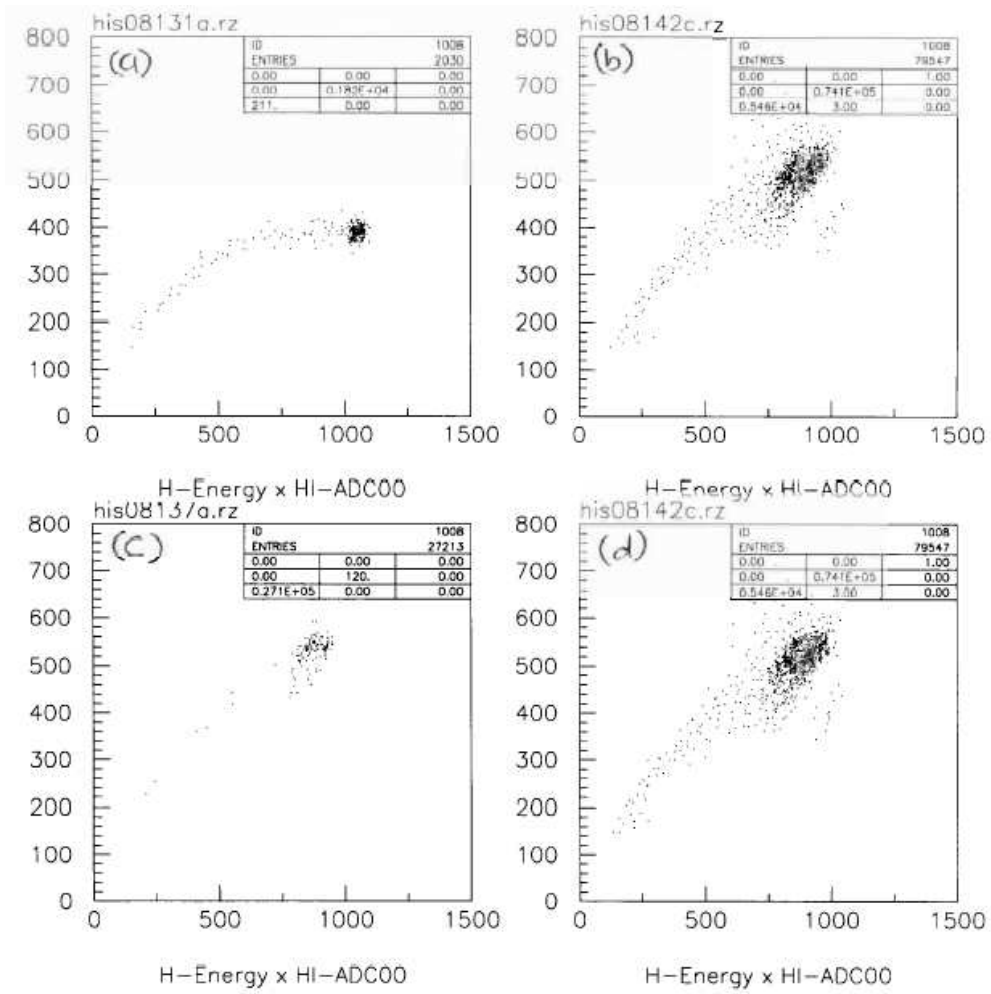


Figure 13: Confirmation of recoils and leaky beam. a) attenuated beam tune, b)+d) normal run, c) recoil tune.

5 Further Analysis

Due to the many excited energy states of ^{14}N , we were to start this analysis by concentrating solely on the 8 MeV ground state gamma emitted in this reaction, which we could compare with Professor Jim King's paper [17].

So how can we separate out the ground state gamma alone?

In a GEANT simulation for 8 MeV gamma rays (figure 14), 82.2% of the number of "hits" made in a single BGO were registered by the PMTs as 8 MeV gammas. Other hits were probably due to random gammas, or 8 MeV gammas which only deposited some of their energy before escaping out of the BGO array. As you can see from figure 15, the array only covers 92% of the solid angle from the gas target, meaning that some gammas escape completely. Looking back at figure 14, 85.3% of the gammas registered, deposited their entire energy in a single BGO. However, 13.9% of the gammas registered, deposited their energy in both a BGO and its neighbor. [12].

Therefore, a method needs to be incorporated into the analyzer, such that an event triggering a BGO, which is then followed by a trigger in a neighboring BGO, registers as an event that we are interested in. But what classifies as a neighboring BGO? As seen in figures 15 and 16, the BGO gamma array is very complex.

The GEANT simulation uses a volume of a cuboid technique, where by if a BGO fires and another fires a certain distance away, which is within the cube, then it classes as a neighboring BGO.

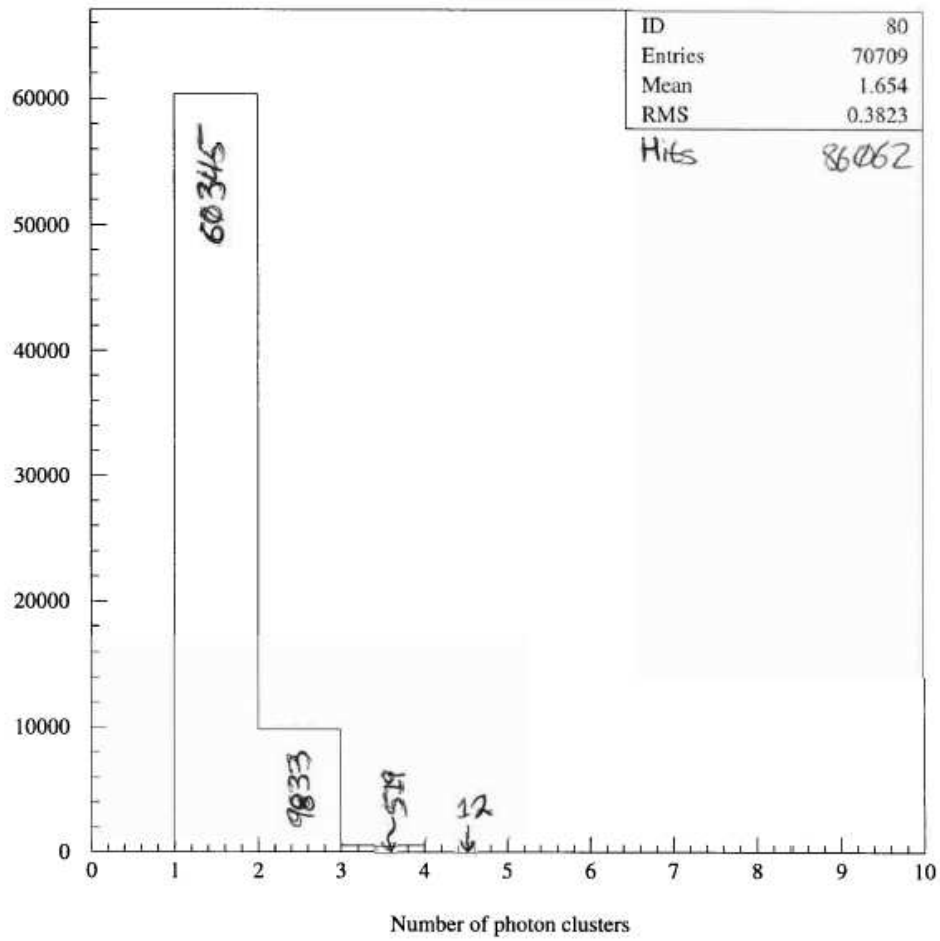


Figure 14: GEANT simulation of the probability of how many of the 8 MeV gammas are deposited in x amount of BGO crystal(s).

GEANT Simulation V.12

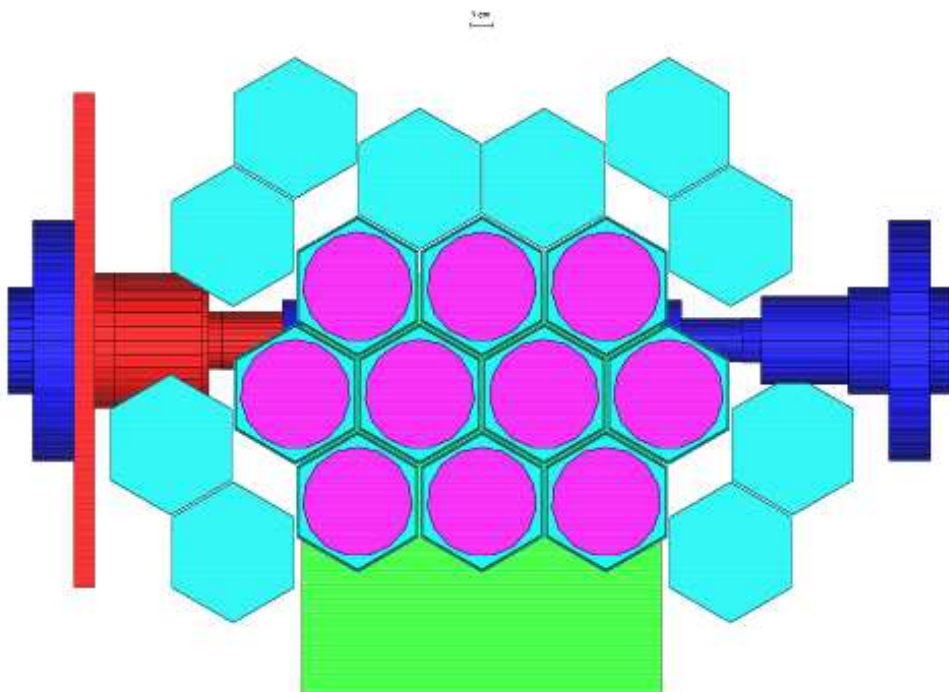


Figure 15: GEANT simulation of the BGO gamma array, looking west of the beam direction.

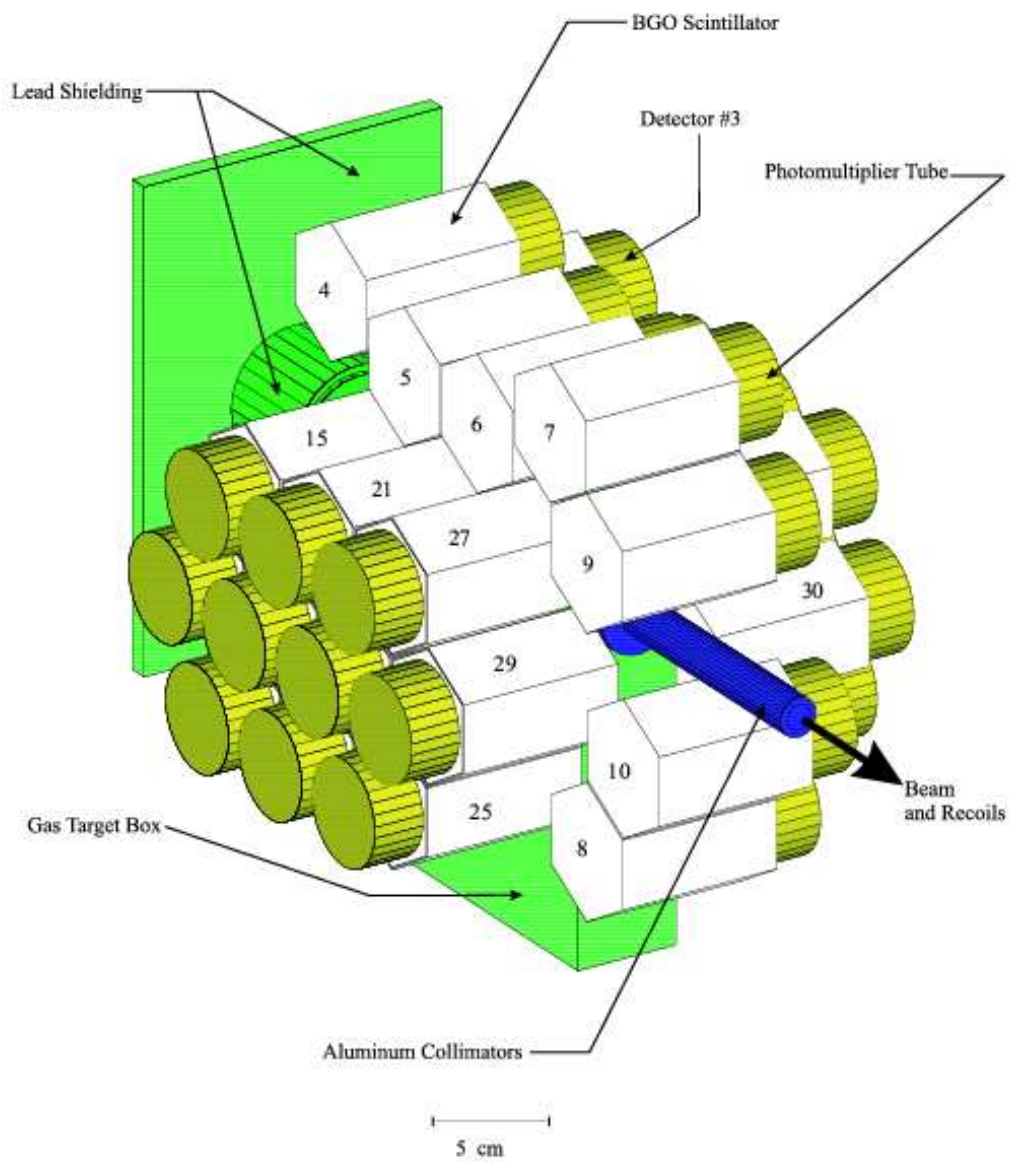


Figure 16: GEANT simulation of a 3D view of the BGO array.

		Neighbouring BGO Detector Array Number																															
		0	1	2	3	4	5	6	7	8	9	10	11	12	13	14	15	16	17	18	19	20	21	22	23	24	25	26	27	28	29		
B	0	0	0	0	0	0	0	0	0	0	1	1	1	0	0	0	0	0	0	0	0	0	0	0	0	0	1	0	1	0	1	0	
G	1	0	0	1	1	0	0	0	0	0	0	0	0	1	1	1	1	1	1	0	0	0	0	0	0	0	0	0	0	0	0	0	
O	2	0	1	0	0	0	0	0	0	0	0	0	0	1	1	1	1	0	0	0	0	0	0	0	0	0	0	0	0	0	0	0	
	3	0	1	0	0	1	1	0	0	0	0	0	0	1	1	0	0	1	1	0	0	0	0	0	0	0	0	0	0	0	0	0	
D	4	0	0	0	1	0	1	0	0	0	0	0	0	0	0	0	0	1	1	0	0	0	0	0	0	0	0	0	0	0	0	0	
e	5	0	0	0	1	1	0	1	0	0	0	0	0	0	0	0	0	1	1	0	0	0	0	1	1	0	0	0	0	0	0	0	
t	6	0	0	0	0	0	1	0	1	0	1	0	0	0	0	0	0	0	0	0	0	0	0	1	1	0	0	0	0	1	1	0	
e	7	0	0	0	0	0	0	1	0	0	1	0	0	0	0	0	0	0	0	0	0	0	0	0	0	0	0	0	0	1	1	0	
c	8	1	0	0	0	0	0	0	0	0	0	0	0	1	0	0	0	0	0	0	0	0	0	0	0	0	0	0	1	1	0	0	1
t	9	1	0	0	0	0	0	1	1	0	0	1	0	0	0	0	0	0	0	0	0	0	0	0	0	0	0	0	0	1	1	1	
o	10	1	0	0	0	0	0	0	0	0	1	1	0	0	0	0	0	0	0	0	0	0	0	0	0	0	0	1	1	1	1	1	
r	11	0	1	1	1	0	0	0	0	0	0	0	0	0	0	1	0	1	0	1	0	0	0	0	0	0	0	0	0	0	0	0	
	12	0	1	1	1	0	0	0	0	0	0	0	0	0	0	1	0	1	0	1	0	0	0	0	0	0	0	0	0	0	0	0	
A	13	0	1	1	0	0	0	0	0	0	0	0	0	1	0	0	0	0	0	1	0	1	0	0	0	0	0	0	0	0	0	0	
r	14	0	1	1	0	0	0	0	0	0	0	0	0	0	0	0	0	0	0	1	0	1	0	0	0	0	0	0	0	0	0	0	
r	15	0	1	0	1	1	1	0	0	0	0	0	0	1	0	0	0	0	0	1	0	0	0	1	0	0	0	0	0	0	0	0	
a	16	0	1	0	1	1	1	0	0	0	0	0	0	0	1	0	0	0	0	0	1	0	0	0	1	0	0	0	0	0	0	0	
y	17	0	0	0	0	0	0	0	0	0	0	0	0	1	0	1	0	1	0	0	0	1	0	1	0	1	0	0	0	0	0	0	
	18	0	0	0	0	0	0	0	0	0	0	0	0	0	0	0	0	0	0	1	0	1	0	1	0	1	0	1	0	0	0	0	
N	19	0	0	0	0	0	0	0	0	0	0	0	0	0	0	0	1	0	0	0	1	0	0	0	0	1	0	1	0	0	0	0	
u	20	0	0	0	0	0	0	0	0	0	0	0	0	0	0	0	0	0	0	1	0	0	0	0	0	0	0	1	0	0	0	0	
m	21	0	0	0	0	0	1	1	0	0	0	0	0	0	0	0	0	1	0	1	0	0	0	0	0	1	0	0	0	1	0	0	
b	22	0	0	0	0	0	1	1	0	0	0	0	0	0	0	0	0	0	1	0	1	0	0	0	0	0	1	0	0	0	1	0	
e	23	0	0	0	0	0	0	0	0	0	0	0	0	0	0	0	0	0	0	1	0	1	0	1	0	0	0	1	0	1	0	1	
r	24	1	0	0	0	0	0	0	0	0	0	0	0	0	0	0	0	0	0	0	1	0	1	0	1	0	0	0	1	0	1	0	
	25	0	0	0	0	0	0	0	0	1	0	1	0	0	0	0	0	0	0	0	0	0	0	1	0	0	0	1	0	0	0	0	1
	26	1	0	0	0	0	0	0	0	1	0	1	0	0	0	0	0	0	0	0	0	0	0	0	0	1	0	0	0	1	0	0	0
	27	0	0	0	0	0	0	1	1	0	1	1	0	0	0	0	0	0	0	0	0	0	0	0	0	1	0	1	0	0	0	0	1
	28	1	0	0	0	0	0	1	1	0	1	1	0	0	0	0	0	0	0	0	0	0	0	0	0	1	0	1	0	0	0	0	0
	29	0	0	0	0	0	0	0	1	1	1	0	0	0	0	0	0	0	0	0	0	0	0	0	0	0	1	0	1	0	1	0	0

Figure 17: An array showing which BGOs are next to each other.

If a neighbor is in fact any BGO that another can “see”, then we can simply create an array (see figure 17) which could be incorporated into our analyzer.

Future plans are:

- 1) to decode previous attempts at this BGO neighboring problem. A C program with ntuples was written and also a GEANT fortran user routine, to compensate for a BGO and its neighbor, but were never used in an analysis.
- 2) to do all the normalization calculations needed, to compare with Professor Jim King’s paper.

3) to create a Monte Carlo simulation to simulate the $^{13}\text{C}(\text{p},\gamma)^{14}\text{N}$ for comparison. Also, we will need to simulate the $^{13}\text{N}(\text{p},\gamma)^{14}\text{O}$ reaction, due to the fact that DRAGON will not be getting the nitrogen beam that they had requested for this year.

4) to modify the DRAGON simulation (currently in the process of being finished) for the $^{13}\text{C}(\text{p},\gamma)^{14}\text{N}$ reaction.

The $^{13}\text{N}(\text{p},\gamma)^{14}\text{O}$ requires quite high sensitivity, so we use the $^{13}\text{C}(\text{p},\gamma)^{14}\text{N}$ reaction to probe the DRAGON not only because it has similar properties, but because it has been measured before by Professor Jim King's group. However, from analysis of our $^{13}\text{C}(\text{p},\gamma)^{14}\text{N}$ run, we see that the ^{14}N recoils are being clipped in the target box. Pure angular clipping⁸ would cause a trough in the coincidence recoil peak, (i.e. giving two peaks), which is what we see in figure 18. However, the left-hand (lower energy) peak should be the same height as the right, as seen in the (uncompleted) DRAGON simulation (figure 19). But we do not see this, and believe the difference in height maybe due to an energy asymmetry correlation problem, whereby low energy recoils are not being focused at the focal point of the end detector. [18].

Once we understand the problems correctly, we can run the finished DRAGON GEANT simulation to see what fraction of the recoils are being cut off, so we can calculate the required parameters such as the yield.

⁸the $^{13}\text{C}(\text{p},\gamma)^{14}\text{N}$ reaction has large maximum cone angle of approximately 90 mrad, which is beyond the design limits of DRAGON (which is approximately 60 mrad) Therefore, some recoils will not make it through the beam line, but are "clipped", staying in the gas target box. [18].

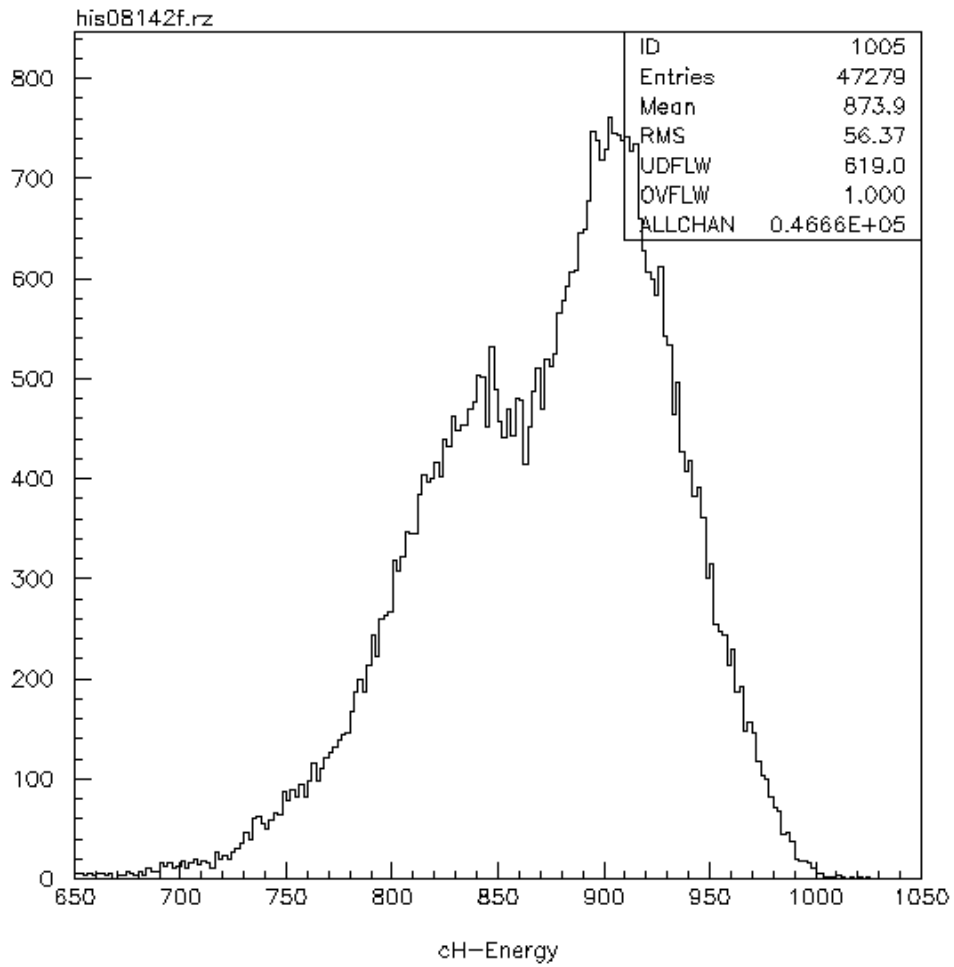


Figure 18: The coincidence recoil spectrum for run 8142, a $^{13}\text{C}(p,\gamma)^{14}\text{N}$ reaction with a incoming beam energy of 558 keV/u.

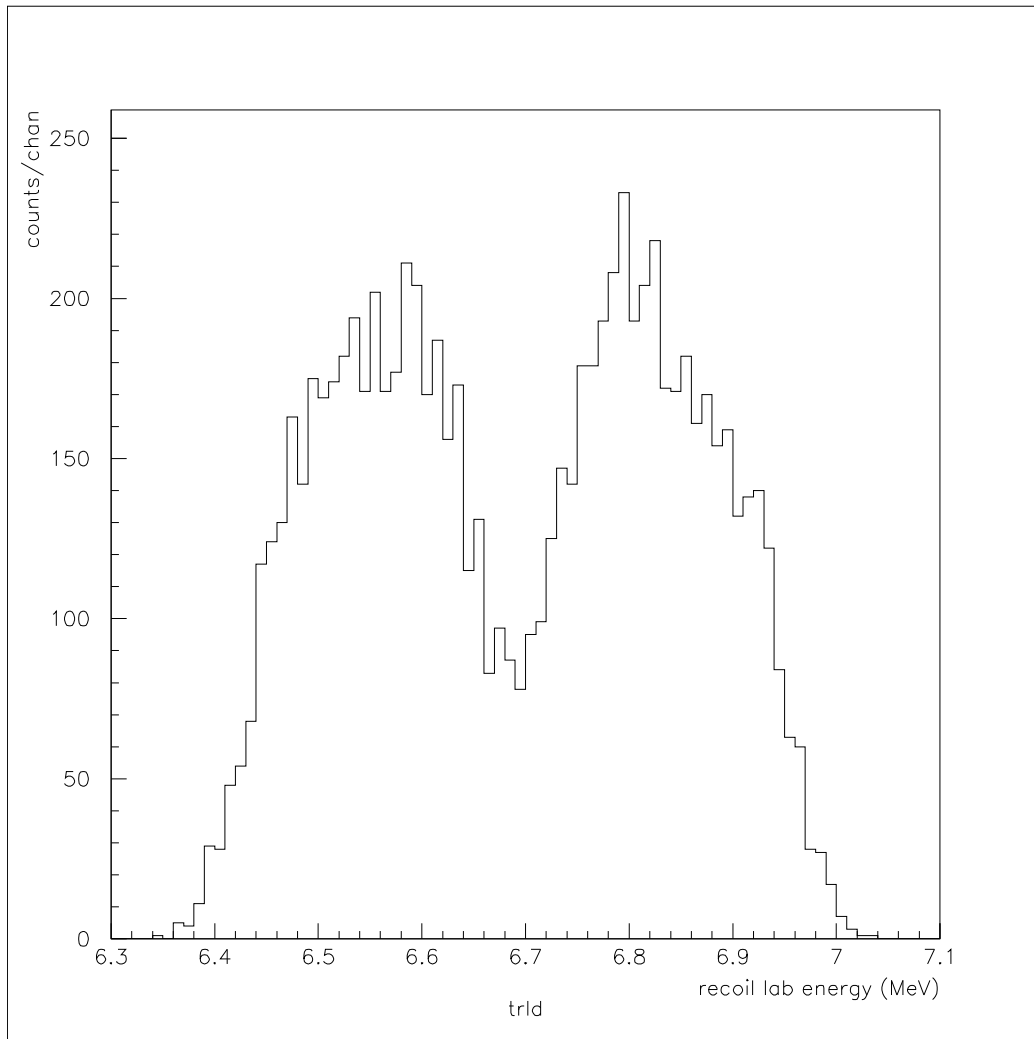


Figure 19: Monte Carlo simulation of the $^{13}\text{C}(p,\gamma)^{14}\text{N}$ reaction with all the gammas plus cascades included, and an angular cut put on the recoils.

6 Conclusion

To conclude, studying the $^{13}\text{C}(\text{p},\gamma)^{14}\text{N}$ reaction is important for the DRAGON facility in their future analysis of the $^{13}\text{N}(\text{p},\gamma)^{14}\text{O}$ reaction, not only due to the similar properties of ^{13}N and ^{13}C , but also as a good test of the DRAGON due to the fact that the $^{13}\text{C}(\text{p},\gamma)^{14}\text{N}$ reaction has been measured before.

Early analysis showed that not all the ^{14}N recoils, from the $^{13}\text{C}(\text{p},\gamma)^{14}\text{N}$ reaction, make it through the DRAGON to the end detector, because they are being clipped in the gas target box.

A GEANT simulation (once finished) will be used to simulate the $^{13}\text{C}(\text{p},\gamma)^{14}\text{N}$ reaction so that we can compare and see what fraction of the recoils are being lost within the DRAGON, and also to see where the clipping occurs.

References

- [1] C. Ruiz, PhD thesis, University of Edinburgh (2003)
- [2] A.Laird, PhD thesis, University of Edinburgh (2000)
- [3] J. Schombert, <http://zebu.uoregon.edu/~js/ast122/lectures/lec11.html>, CNO Cycle
- [4] A. E. Champagne and M. Wiescher, *Ann. Rev. Nucl. Part. Sci.* **42** (1992) 39
- [5] A. Endo et al., www.irpa.net/irpa10/cdrom/00660.pdf, Charaterization of ^{11}C , ^{13}N , and ^{15}O produced in Air through Nuclear Spallation Reactions by High Energy protons
- [6] www.triumf.ca/welcome/about.html, About TRIUMF
- [7] www.triumf.ca/isac/bluepost1.pdf, The ISAC Radioactive Beam Facility in Canada: Progress and Plans
- [8] A. Chen, www.triumf.ca/isac/chenweb.pdf, ISAC: Radioactive Beams at TRIUMF
- [9] C. Neish, <http://www.triumf.ca/dragon/system.html>, The DRAGON System, (2003)
- [10] C. Neish (2003), Novae in a test-tube: Investigating the $^{21}\text{Na}(p,\gamma)^{22}\text{Mg}$ reaction at TRIUMF's ISAC facility, (Final report, internal)
- [11] D.Hutcheon et al., *Nuclear Instruments and Methods in Physics Research A* **498** (2003) 190-210

- [12] D. Gigliotti, Master's thesis, University Of Northern British Columbia (in preparation) (2003)
- [13] C. Wrede, Master's thesis, Simon Fraser University (in preparation) (2003)
- [14] S. McGee, D. Hunter, (2001), Parallel Grid Avalanche Counter, (Final report, internal)
- [15] P. Amaudraz, <http://pierre.triumf.ca/midas/intro.html>, What is MIDAS?
- [16] J. Rogers, http://www.triumf.ca/dragon/MIDAS_analyzer.html, The DRAGON/MIDAS Analyser, (2003)
- [17] J. King et al., Nuclear Physics A 567 (1994) 354-376
- [18] C. Ruiz, private communication (2003)